Model of level statistics for disordered interacting quantum many-body systems

Piotr Sierant[1,2,*] and Jakub Zakrzewski[1,3,†]

[1]*Institute of Theoretical Physics, Jagiellonian University in Krakow, Łojasiewicza 11, 30-348 Kraków, Poland*
[2]*Institut de Sciences Fotoniques, The Barcelona Institute of Science and Technology, 08860 Castelldefels (Barcelona), Spain*
[3]*Mark Kac Complex Systems Research Center, Jagiellonian University in Krakow, 30-348 Kraków, Poland*

(Received 30 July 2019; revised manuscript received 21 February 2020; accepted 21 February 2020; published 11 March 2020)

We numerically study level statistics of disordered interacting quantum many-body systems. A two-parameter plasma model which controls the level repulsion exponent β and range h of interactions between eigenvalues is shown to reproduce accurately features of level statistics across the transition from the ergodic to many-body localized phase. Analysis of higher-order spacing ratios indicates that the considered β-h model accounts even for long-range spectral correlations and allows us to obtain a clear picture of the flow of level statistics across the transition. Comparing the spectral form factors of the β-h model and of a system across the ergodic-many-body-localized transition, we show that the range of effective interactions between eigenvalues h is related to the Thouless time which marks the onset of quantum chaotic behavior of the system. Analysis of level statistics of the random quantum circuit which hosts chaotic and localized phases supports the claim that the β-h model grasps universal features of level statistics in transition between ergodic and many-body-localized phases also for systems breaking time-reversal invariance.

DOI: 10.1103/PhysRevB.101.104201

I. INTRODUCTION

Many-body localization (MBL) [1,2] manifesting ergodicity breaking in disordered interacting quantum many-body systems [3–6] has attracted vivid attention over the last decade. Important results include an emergent integrability of the MBL phase due to the existence of local integrals of motion (LIOMs) [3,7–10] and the associated logarithmic growth of the bipartite entanglement entropy after a quench from a separable state [11,12]. A wide regime of subdiffusive transport on the ergodic side of the transition was found [13–15]. Signatures of MBL have been observed experimentally in one-dimensional (1D) [16,17] and two-dimensional [18] systems (see, however, [19]). Recently, the very existence of MBL in the thermodynamic limit has been questioned [20], opening a new debate [21–23]. While the status of MBL in the thermodynamic limit is of utmost importance for the understanding of this phenomenon from a purely theoretical viewpoint, the real systems studied in this respect are finite [16,18,24,25], often reaching very modest sizes that enable precise studies [26–28]. In this work we concentrate on systems of such a size.

Spectral statistics of ergodic systems with and without time-reversal invariance follow predictions of a Gaussian orthogonal ensemble (GOE) and a Gaussian unitary ensemble (GUE), respectively, of random matrices [29,30], while eigenvalues of localized systems are uncorrelated, resulting in Poisson statistics (PS). A ratio of consecutive spacings between energy levels

$$r_i^{(n)} = \min\left\{\frac{E_{i+2n}-E_{i+n}}{E_{i+n}-E_i}, \frac{E_{i+n}-E_i}{E_{i+2n}-E_{i+n}}\right\} \tag{1}$$

was proposed as a simple probe of the level statistics in [31] with $n = 1$ and employed in the investigation of ergodicity breaking in various settings [32–40]. Higher-order spacing ratios ($n > 1$), studied in [41–45], are valuable tools to assess the properties of level statistics. In contrast to standard measures such as level spacing distribution and number variance [29,30] they do not require the so-called unfolding, i.e., the procedure of setting the density of energy levels $\rho(E)$ to unity, which can lead to misleading results [46]. Recently, an analytical understanding of the appearance of random matrix theory statistics in systems without a clear semiclassical limit was developed in a periodically driven Ising model [47,48] and in random Floquet circuits [49]. Variants of such systems have been argued to undergo ergodic-MBL transition [50,51].

In this work we introduce a two-parameter β-h model which assumes a level repulsion determined by the exponent β between h neighboring eigenvalues. Our model is a natural extension of the so-called β-Gaussian model [45] claimed to represent the level statistics in the transition to MBL. We show that the second parameter, the interaction distance h, is essential for understanding the transition and reproducing the numerical results obtained for various physical models. In particular, we demonstrate that distributions of higher-order spacing ratios $r^{(n)}$ across the ergodic-MBL transition in the disordered XXZ spin chain are faithfully captured by the β-h model and the obtained β and h parameters provide a simple perspective on short-range and long-range spectral correlations. The latter, captured effectively by the interaction range h, are further investigated by means of the spectral form

*piotr.sierant@uj.edu.pl
†jakub.zakrzewski@uj.edu.pl

factor (SFF), revealing a link between h and the Thouless time. We demonstrate that the β-Gaussian model fails to describe long-range spectral correlations. An analysis of a local Haar-random unitary nearest-neighbor quantum circuit system introduced in [50] indicates that in such a generic system the spectral statistics can also be grasped with the β-h model, demonstrating the robustness of the observed features of level statistics.

This paper is organized as follows. In Sec. II we introduce the β-h model and discuss the properties of its level statistics. In Sec. III we show that the β-h model accurately reproduces level statistics of the disordered XXZ spin chain across the many-body localization transition. In Sec. IV we show that the β-h model also grasps level statistics of the disordered Bose-Hubbard model. In Sec. V we demonstrate that β-h also applies to the ergodic-MBL transition in systems with broken time-reversal symmetry and without local conservation laws by considering level statistics of a random quantum circuit. We conclude in Sec. VI.

II. THE β-h MODEL

The joint probability density function (JPDF) of eigenvalues of the matrix from GOE (GUE) with $\beta = 1$ ($\beta = 2$) can be written as a partition function of a fictitious 1D gas of particles $\mathcal{P}(E_1, \ldots, E_N) = Z_N^{-1} \mathrm{e}^{-\beta \mathcal{E}(E_1,\ldots,E_N)}$, where Z_N is a normalization constant and the energy $\mathcal{E}$ includes a trapping potential $U(E) \propto E^2$ and pairwise logarithmic interactions $V(|E - E'|) = -\ln(|E - E'|)$. Eigenvalues $E_1 < \cdots < E_N$ lie on a ring of length N which confines them, rendering the trapping potential $U(E)$ unnecessary. The JPDF can be written as

$$\mathcal{P}_h^{\beta}(E_1, \ldots, E_N) = Z_N^{-1} \prod_{i=0}^{N} |E_i - E_{i+1}|^{\beta} \cdots |E_i - E_{i+h}|^{\beta}. \tag{2}$$

The GOE (GUE) case is obtained when $h \to \infty$ with the appropriate value of β. The form of (2) suggests various models of intermediate level statistics between GOE (GUE) and PS. For instance, one can keep $h \to \infty$ and vary β, obtaining the so-called β-Gaussian ensemble [45]. When h is an integer number which sets the number of correlated neighboring eigenvalues, one arrives at the so-called short-range plasma model introduced in [52] (see also [53,54]).

In this work we extend this model by allowing h to be a real number. Denoting by $\lfloor . \rfloor$ the floor function, the factor in (2) becomes $|E_i - E_{i+1}|^{\beta} \cdots |E_i - E_{i+\lfloor h \rfloor}|^{\beta} |E_i - E_{i+\lfloor h \rfloor+1}|^{\beta(h-\lfloor h \rfloor)}$, hence defining the β-h model where $h \in [1, \infty)$ and $\beta \in [0, 1]$ ($\beta \in [0, 2]$) for GOE- (GUE-) PS transition. Varying continuously h and β allows us to capture spectral statistics of disordered quantum many-body systems across the ergodic-MBL transition, while a simple form of the JDPF of the β-h model yields insight into correlations between eigenvalues. Semianalytical results for the β-h model are available only for integer values of h and β [52]. In particular, the number variance, defined as the variance of the number of eigenvalues in an interval $(E, E + L)$, reads

$$\Sigma^2(L) = \chi L \tag{3}$$

for $L \gg 1$, where $\chi = 1/(\beta h + 1)$. The spectral rigidity of GOE (GUE) which manifests itself in the logarithmic growth of the variance $\Sigma^2(L)$ is replaced by a finite spectral compressibility χ. Thus, a profound change in long-range spectral correlations happens when $h < \infty$. Interestingly, we find that (3) is fulfilled with excellent agreement with the β-h model, as our Monte Carlo simulations (obtained sampling the JPDF of the β-h model with the Metropolis-Hastings algorithm [55]) show for arbitrary real $\beta \in [0, 2]$ and $h \in [1, 40]$.

A straightforward application of the method of [52] shows that distributions of higher-order spacing ratios $P(r^{(n)})$ for $h = 1$ are given by

$$P(r^{(n)}) = \mathcal{N}_{n,\beta} \frac{(r^{(n)})^{\beta+(n-1)(\beta+1)}}{(1 + r^{(n)})^{2(\beta+1)n}}, \tag{4}$$

where $\mathcal{N}_{n,\beta} = [{}_2F_1(n(1+\beta), 2n(1+\beta), 1 + n(\beta+1), -1)/(\beta+1)n]^{-1}$ is a normalization constant and ${}_2F_1$ is Gauss hypergeometric function. Such distributions of higher-order spacing ratios $P(r^{(n)})$ at $h = 1$ constitute a very good approximation for systems close to the MBL phase where $h \approx 1$ and provide analytical expressions for average higher-order spacing ratios $\bar{r}^{(n)}$ (including PS for $\beta = 0$). To obtain $P(r^{(n)})$ for arbitrary $h \in [1, \infty)$ and $\beta \in [0, 1]$ we again sample the JPDF of the β-h model with the Monte Carlo approach.

A. Spectral form factor of the β-h model

Consider the *spectral form factor* [29,30]:

$$K(\tau) = \frac{1}{Z} \left\langle \left| \sum_j g(\epsilon_j) \mathrm{e}^{-iE_j\tau} \right|^2 \right\rangle, \tag{5}$$

where Z ensures that $K(\tau) \overset{\tau\to\infty}{\to} 1$, the spectrum is unfolded (for remarks on unfolding see the Appendix), and $g(\epsilon)$ is a Gaussian function which vanishes at the edges of the spectrum, reducing their influence (see also the Appendix). The SFF allows us to identify two important timescales in disordered systems: the Heisenberg time τ_H equal to the inverse level spacing, beyond which the discrete nature of the energy spectrum manifests itself, and the Thouless time τ_{Th}, which is the timescale beyond which SFF admits universal GOE (GUE) form $K(\tau) \approx 2\tau$ [20,50]. The existence of two timescales is reflected in the JPDF of the β-h model, where the correlations between eigenvalues are of the GOE (GUE) form on energy scales smaller than h level spacings so that τ_{Th}, inversely proportional to h (for $\beta = 1, 2$), provides a physical interpretation of the interaction range h in the β-h model.

The SFF of the β-h model is shown in Fig. 1. For $\beta = 1$, the SFF of the β-h model follows the prediction for GOE down to Thouless time τ_{Th}, which depends on the interaction range h [roughly, $\tau_{\mathrm{Th}} \approx 2/(h+1)$]. The SFF for $\beta < 1$ shows that it is possible to have spectral statistics with $h > 1$ and $\tau_{\mathrm{Th}} = \tau_H = 1$.

We note that (3) implies that $K(0) = 1/(\beta h + 1)$, an analytical prediction for integer β and h which is very well confirmed by numerical data for arbitrary β and h, as shown in Fig. 1.

Figure 2 shows a comparison of SFFs of the β-h model and of the β-Gaussian ensemble. The two parameters of the β-h model allow us to reproduce the typical behavior

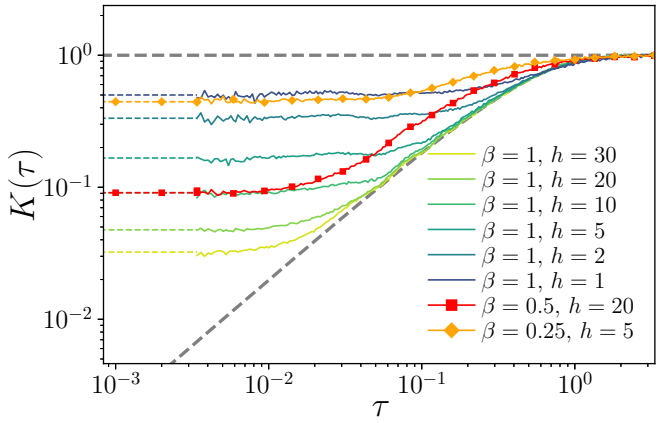

FIG. 1. The SFF $K(\tau)$ of the β-h model. For $\tau < 0.003$, $K(\tau)$ was replaced by an analytically determined value of $K(0)$. Gray dashed lines correspond to GOE and PS.

of the SFF of a disordered many-body system across the ergodic-MBL transition [20,22]—the Thouless time $t_{\rm Th}$ of a physical quantum many-body system increases with disorder strength W, which, in the β-h model is reflected by a decreasing range h of eigenvalue interactions. The vanishing level repulsion in the vicinity of the localized phase is reflected by a sufficiently small value of the exponent β. This is not the case for the β-Gaussian ensemble. As soon as $\beta < 1$, the deviation from the SFF of GOE is observed for all $\tau < 1$, as Fig. 2 illustrates. Thus, the β-Gaussian ensemble is unable to reproduce the typical behavior of the SFF $K(\tau)$ in a disordered system in which $K(\tau)$ deviates from the universal GOE curve only for times smaller than the Thouless time $t_{\rm Th}$. Moreover, for $\beta < 1$ the predictions of the β-Gaussian ensemble fail to reproduce a small τ behavior, showing a rapid decrease with decreasing τ instead of a saturation as expected closer to the Poisson regime.

III. XXZ SPIN CHAIN

Let us go beyond a comparison of the statistical models among themselves and compare their predictions with differ-

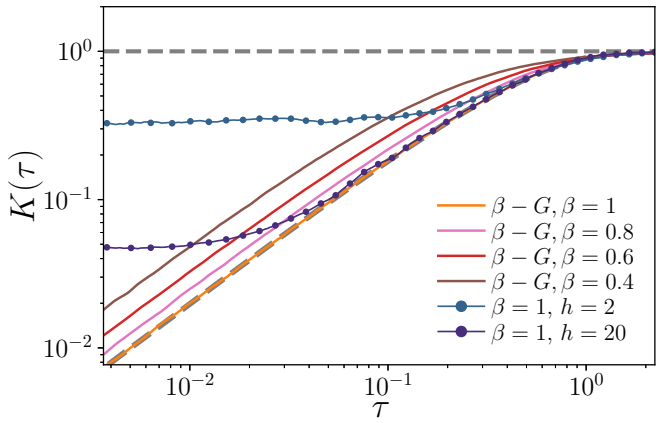

FIG. 2. Comparison of SFFs of the β-h model (lines with dots) and of the β-Gaussian ensemble (solid lines). Gray dashed lines correspond to GOE and PS.

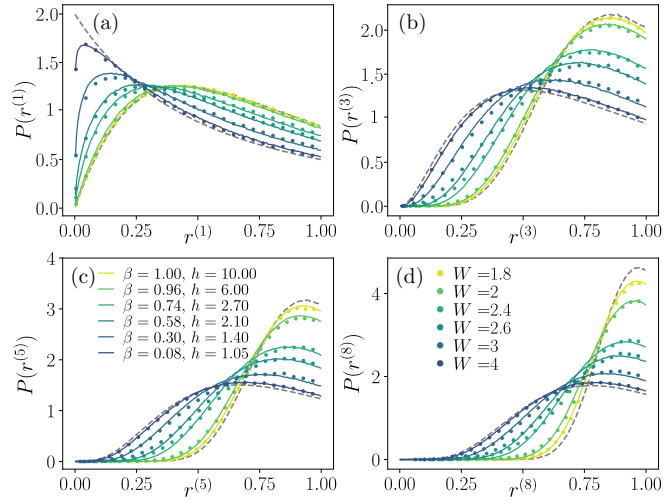

FIG. 3. Distributions of higher-order spacing ratios of the disordered XXZ spin chain (6) of size $L = 18$ for various disorder strengths W are denoted by symbols. Lines correspond to the β-h model with parameters shown in (c). Gray dashed lines correspond to $P(r^{(n)})$ distributions for GOE and PS.

ent physical models. As a starting point for testing purposes we consider a standard disordered XXZ spin-1/2 chain with the Hamiltonian given by

$$H = J \sum_{i=1}^{L} \vec{S}_i \cdot \vec{S}_{i+1} + \sum_{i=1}^{L} h_i S_i^z, \tag{6}$$

where $\vec{S}_i$ are spin-1/2 matrices; $J = 1$ is fixed as the energy unit; periodic boundary conditions are assumed, $\vec{S}_{L+1} = \vec{S}_1$; and $h_i \in [-W, W]$ are independent, uniformly distributed random variables. The model (6) has been widely studied in the MBL context [11,32,35,56–62], and its level statistics were addressed in [63–66]. Recently, the β-Gaussian ensemble was suggested to describe the ergodic-MBL transition [45]. As the analysis in Sec. II showed, this claim is questionable. Further, we shall show that the β-Gaussian ensemble reproduces level correlations only on a single-level spacing scale while missing longer-range spectral correlations. Both aspects of level statistics are grasped by the β-h model.

Eigenvalues of the XXZ spin chain (6) are obtained by an exact diagonalization for small sizes or with the shift-and-invert method [67] for $L = 18, 20$. For each W we accumulate eigenvalues from 2000 (400) disorder realizations for $L \leqslant 18$ ($L = 20$). The higher-order spacing ratios (1) are calculated using 500 eigenvalues from the middle of the spectrum. The resulting exemplary distributions $P(r^{(n)})$ of higher-order spacing ratios for $n = 1, 3, 5, 8$ are shown in Fig. 3. Parameters for the β-h model are obtained by minimizing the deviation between $P(r^{(n)})$ distributions for the XXZ spin chain and the β-h model. Very good agreement between the distributions obtained for the model (6) and predictions of the β-h model is observed in the whole transition region between the ergodic and MBL phases. Note that both parameters β and h are needed to reproduce $P(r^{(n)})$ distributions for $n \geqslant 1$. To demonstrate that the agreement between the β-h model and level statistics of the XXZ spin chain in

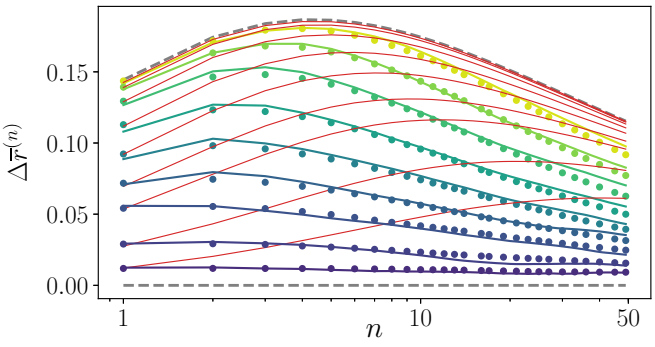

FIG. 4. Symbols show the average higher-order gap ratios $\Delta\bar{r}^{(n)}$ (see text) as s function of n for disorder strengths $W = 1.8, 2, 2.2, 2.4, 2.6, 2.8, 3, 3.4, 4$ (from top to bottom) for an XXZ chain of size $L = 18$. Corresponding fits of the β-h model are drawn by solid lines; the β and h parameters are the same as in Fig. 3, and additional $W = 2.2, 2.8, 3.4$ are fitted by $\beta = 0.90, 0.46, 0.18$ and $h = 3.60, 1.70, 1.30$, respectively. Red lines correspond to the β-Gaussian ensemble with $\beta = 0.98, 0.94, 0.84, 0.68, 0.52, 0.38, 0.26, 0.12, 0.05$ (from top to bottom). Gray dashed lines show $\Delta\bar{r}^{(n)}$ for GOE and PS.

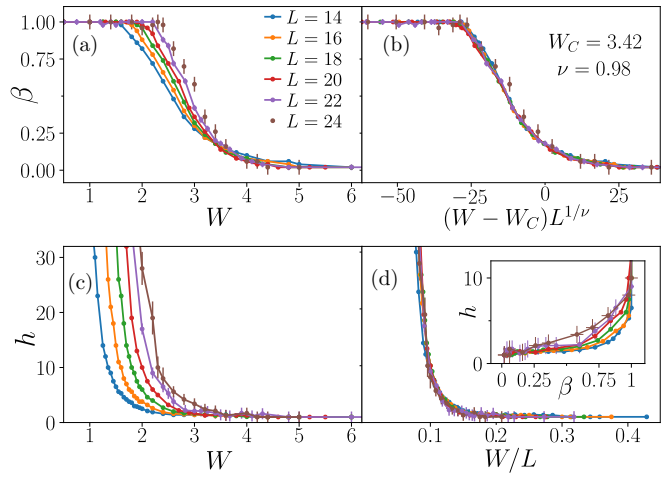

FIG. 5. (a) Level repulsion exponent β and (c) the range h of interactions of eigenvalues as a function of disorder strength W in the XXZ chain. The collapse of the data (b) for $\beta(W)$ upon rescaling $W \to (W - W_C)L^{1/\nu}$ and (d) for $h(W)$ using $W \to W/L$ rescaling. The inset in (d) shows the dependence $h(\beta)$ for various system sizes.

ergodic-MBL crossover persists to larger energy scales, we calculate $\Delta\bar{r}^{(n)} = \bar{r}^{(n)} - \bar{r}^{(n)}_{PS}$, where $\bar{r}^{(n)}$ is the average value of the nth-order spacing ratio $\bar{r}^{(n)}$ and $\bar{r}^{(n)}_{PS}$ is the nth-order average gap ratio for PS. The resulting values of $\Delta\bar{r}^{(n)}$ as a function of n are shown in Fig. 4. Even though the parameters of the β-h model are determined by the fit of $P(r^{(n)})$ for only $n = 1, 3, 5, 8$ (fits for all n are taken with the same weight), the good agreement between $\Delta\bar{r}^{(n)}$ for the XXZ spin chain and for the β-h model persists up to $n = 50$. Interestingly, on the ergodic side of the transition, for $W \leqslant 2.4$, the values of $\Delta\bar{r}^{(n)}$ for $n \geqslant 20$ predicted by the β-h model consequently overestimate the values for the XXZ spin chain. Since the larger value of $\Delta\bar{r}^{(n)}$ implies stronger level correlations at the scale determined by n, this means that energy levels of the β-h model, not coupled directly in the JPDF (6), are still correlated more strongly than energy levels of the system across the ergodic-MBL transition. For comparison, we also show the predictions of the β-Gaussian ensemble [45] in Fig. 4. Only the values of $\Delta\bar{r}^{(1)}$ are well reproduced by this approach; for $n \geqslant 2$, the values of $\Delta\bar{r}^{(n)}$ are overestimated, showing that finite h is an essential feature of level statistics in the MBL transition.

A. Scaling of the level repulsion exponent β and range of interactions h at the ergodic-MBL transition

The β and h parameters characterizing level statistics across the ergodic-MBL transition are shown in Fig. 5. In the ergodic phase, at small disorder strengths W, GOE describes level statistics well; hence, $\beta = 1$ and $h \to \infty$. Upon increasing W, the range of interactions h and the level repulsion exponent β decrease, leading to PS for sufficiently strong disorder. Notably, the system size dependences of $h(W)$ and $\beta(W)$ are very different. The data for $\beta(W)$ collapse upon rescaling $W \to (W - W_C)L^{1/\nu}$ with $W_C \approx 3.4$ and $\nu \approx 1$, similar to the average gap ratio $\bar{r}^{(1)}$ [35], indicating that $\bar{r}^{(1)}(W)$ and $\beta(W)$ contain similar information. In particular, both measures lead to the exponent $\nu < 2$, violating the Harris bound [68–70]. On the other hand, data for $h(W)$ collapse upon rescaling $W \to W/L$. As the inset in Fig. 5(d) demonstrates, the decrease of the level repulsion exponent β in the transition region is accompanied by the interaction range h increasing with L for a given value of β. Therefore, our data indicate the presence of the transition to the MBL phase with vanishing level repulsion exponent $\beta = 0$ at disorder strength W_C even though the interaction range admits a certain fixed value $h_0 = h(W^*)$ at disorder strength W^* increasing linearly with the system size L. The linear dependence $W^* \sim L$ persists steadily up to the largest available system size $L = 24$, but since the values of h in the transition region do not exceed 10, we cannot conclude whether h diverges or stays finite at the transition in the thermodynamic limit. Nevertheless, in either case, the level repulsion vanishes at the transition in the $L \to \infty$ limit, in accordance with recent phenomenological treatments [71,72]. We note that a linear with system size dependence for the deviation of $\bar{r}^{(1)}$ from the value characteristic for GOE was found recently in [20]. This observation is related to our finding that $W^* \sim L$ since disorder strength for which h becomes of the order of, e.g., $h_0 = 10$ is, at the same time, the moment for which $\bar{r}^{(1)}$ departs from the value characteristic for GOE. While the β-h model puts the long-range spectral statistics examined in [20] in another perspective, we emphasize that the presented data suggest a transition to the MBL phase at disorder strength W_C in the thermodynamic limit.

B. The spectral form factor of the XXZ spin chain

Let us now consider the SFF of the XXZ spin chain, which is shown in Fig. 6 along with the predictions of the β-h model. Beyond the Heisenberg time τ_H, $K(\tau) = 1$. For smaller τ, the SFF of the XXZ spin chain follows the GOE prediction down to the Thouless time $\tau_{\rm Th}$, which increases monotonically with disorder strength W. The behavior is captured by the SFF of the β-h model. For $\tau < \tau_{\rm Th}$, an increase in the SFF of the XXZ

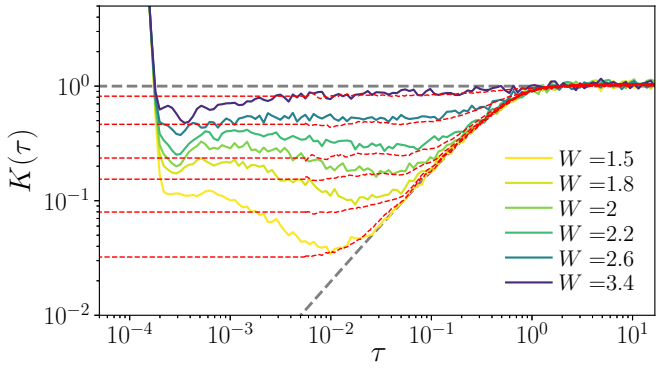

FIG. 6. SFF for system (5) of size $L = 18$ for various disorder strengths W. Predictions of the β-h model with the same parameters as in Fig. 4 (data for $W = 1.5$ fitted with $\beta = 1, h = 30$) are denoted by red dashed lines (for $\tau < 0.005$ SFF was replaced by the exact value in $\tau = 0$). Gray dashed lines correspond to GOE and PS.

chain is observed for disorder strengths W corresponding to the ergodic side of the transition, whereas the SFF remains constant for the β-h model. The latter behavior signals weak correlations between eigenvalues of the β-h model beyond energy scale determined by h, whereas the behavior of the SFF of the XXZ spin chain indicates even weaker correlations of its eigenvalues.

C. Level statistics and number variance across the ergodic-MBL transition

We revisit now the level spacing distribution and the number variance of the disordered XXZ spin chain in the ergodic-MBL crossover, shown in Fig. 7. Level spacing distributions are very faithfully reproduced by the β-h model in the whole crossover regime. There are, however, slight deviations in the number variance $\Sigma^2(L)$ of the XXZ spin chain and the β-h model. On the ergodic side of the crossover ($W < 2.4$) the β-h model underestimates the number variance of the XXZ spin chain, indicating weaker long-range spectral correlations of the latter, in agreement with the analysis of $\Delta\bar{r}^{(n)}$ in this regime. For large W, the prediction of the β-h model overestimates the number variance of the XXZ spin chain, which is probably related to the effects of a finite number of eigenvalues n_e from a single disorder realization, which are known to contribute as $-L^2/n_e$ to the number variance $\Sigma^2(L)$ [66].

We note that results for the number variance $\Sigma^2(L)$ are strongly dependent on the way the level unfolding is performed; in view of that we conclude that the higher-order spacing ratios are more reliable in extracting information about spectral correlations beyond single-level spacing. Furthermore, when one inspects tails $s \gtrsim 4$ of the level spacing distribution on the logarithmic scale, deviations from predictions of the β-h model are found. As demonstrated in [66], such behavior at large s is associated with the large intersample randomness associated with the ergodic-MBL transition in random potentials.

The weighted short-range plasma model for level statistics in the ergodic-MBL crossover was considered in [66]. This model takes into account intersample randomness, an

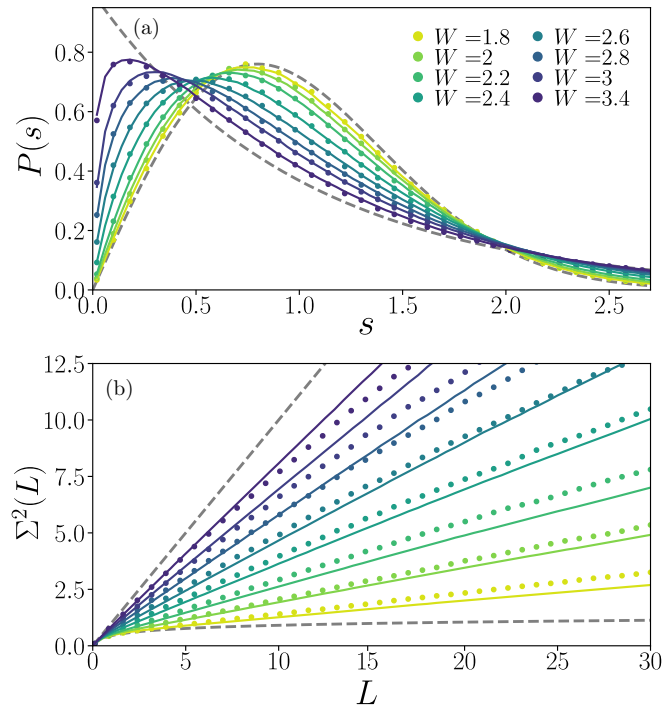

FIG. 7. (a) Level spacing distributions $P(s)$ of the XXZ spin chain of size $L = 18$ for various disorder strengths W are denoted by markers. Lines correspond to predictions of the β-h model with parameters as in the main text. (b) Number variance $\Sigma^2(L)$ of the XXZ spin chain and prediction of the β-h model.

important feature of the MBL transition in random potentials [73]. The JPDF of the weighted short-range plasma model is a weighted superposition of the JPDF of the form (2), and as such, it is related to the β-h model. However, the necessity of reproducing the intersample randomness requires an introduction of many weight parameters. This makes using the weighted short-range plasma model complicated. The simple picture of changes in interaction range between eigenvalues and its relation to Thouless time cannot be easily extracted due to the complexity of the model. It must be noted, however, that taking into account the intersample randomness determined by a sample-averaged spacing ratio [66] could diminish the (small) deviations in $P(r^{(n)})$ between the β-h model and the XXZ spin chain for disorder strengths $W = 2.4, 2.6$, for which the intersample randomness is the largest at $L = 18$.

A two-stage [63] picture of the flow of level statistics between GOE and PS proposes that on the ergodic side of the crossover level statistics are described by a plasma model with power-law interactions between eigenvalues which yields the following expressions for the level spacing distribution and the number variance:

$$P(s) = C_1 s^{\beta} \mathrm{e}^{-C_2 s^{2-\gamma}}, \quad \Sigma_2(L) \propto L^{\gamma}, \tag{7}$$

with $C_{1,2}$ determined by normalization conditions $\langle 1 \rangle = \langle s \rangle = 1$. The exponents β and γ play a role similar to the β and h parameters of the β-h model. In the transition from the extended to the localized regime in the first stage γ changes from 0 to 1, leading to a Poissonian tail of $P(s)$ followed, at the second stage, by a change in level repulsion β. However,

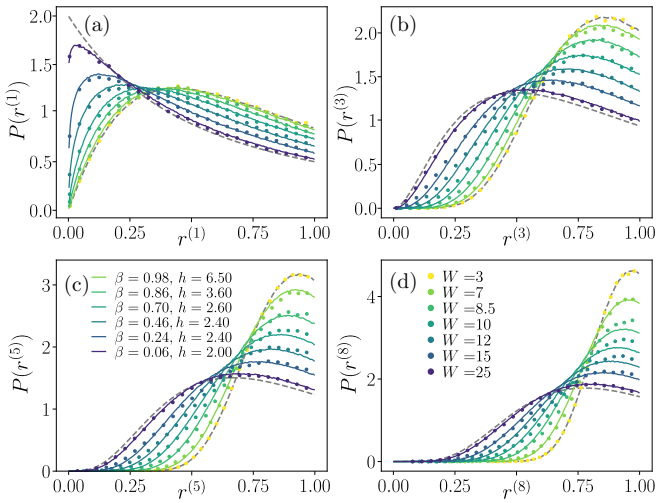

FIG. 8. Distributions of higher-order spacing ratios for the Bose-Hubbard model (8) of size $L = 8$ with $N = 12$ particles are denoted by markers; fits of the β-h model to data with $W \geqslant 7$ are denoted by solid lines. Higher-order spacings distributions ($n = 1, 3, 5, 8$) for $W = 3$ are indistinguishable from appropriate distributions for GOE. Dashed lines correspond to GOE and PS.

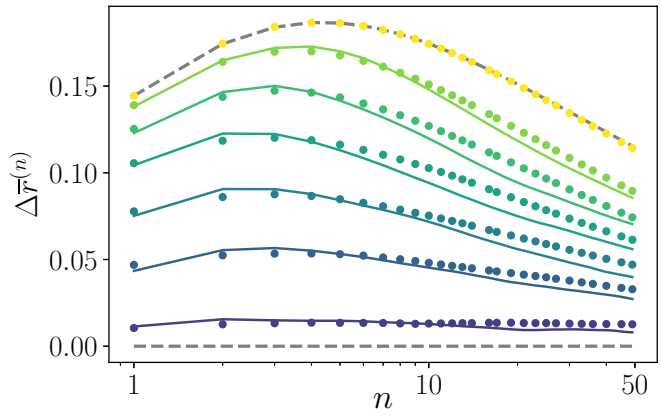

FIG. 9. Average higher-order spacing ratios for the Bose-Hubbard model with disorder strengths $W = 3, 7, 8.5, 10, 12, 15, 25$ (from top to bottom) denoted by markers; predictions of the β-h model fitted to data with $W \geqslant 7$ with the same parameters as in Fig. 8 are denoted by solid lines. Level statistics for $W = 3$ are indistinguishable from GOE statistics on the considered energy scale. Gray dashed lines correspond to GOE and PS.

as demonstrated in [64], the predictions of (7) are not valid as the number variance $\Sigma^2(L)$ in the ergodic-MBL transition grows linearly (or superlinearly; see Fig. 7), contrary to the prediction of (7) where $0 < \gamma < 1$ in the crossover regime. Moreover, (7) is obtained on the mean-field level [74]; no other predictions for this model such as the JPDF are available. The second stage of the flow [63] coincides with the β-h model with $h = 1$. However, as shown above, the $h(\beta)$ dependence is such that the interaction range h for a fixed value of β is increasing; hence, h becomes equal to unity only deep in the MBL regime.

IV. LEVEL STATISTICS OF THE DISORDERED BOSE-HUBBARD MODEL

To provide further evidence that the β-h model is able to reproduce level statistics of interacting disordered quantum many-body systems, we analyze higher-order spacing ratios in the ergodic-MBL transition in a disordered Bose-Hubbard model [75,76] with the Hamiltonian

$$H_B = -J \sum_{\langle i,j \rangle} \hat{a}_i^\dagger \hat{a}_j + \frac{U}{2} \sum_i \hat{n}_i(\hat{n}_i - 1) + \sum_i \mu_i \hat{n}_i, \qquad (8)$$

where $a_i^\dagger, a_i$ are bosonic creation and annihilation operators, respectively, the tunneling amplitude $J = 1$ sets the energy scale, $U = 1$ is the interaction strength, and the chemical potential μ_i is distributed uniformly in the interval $[-W; W]$. This model undergoes a transition to MBL phase beyond critical disorder strength W_C, which depends on the interaction strength U.

Distributions of higher-order spacing ratios ($n = 1, 3, 5, 8$) for the disordered Bose-Hubbard model are shown in Fig. 8. The β-h model faithfully reproduces distributions $P(r^{(n)})$ in the whole crossover regime. We note that the dependence $h(\beta)$ is markedly different compared to the XXZ spin chain; here we find $h = 2$ even when the level repulsion exponent β is close to zero. Average higher-order spacing ratios shown in Fig. 9 indicate that long-range spectral statistics are also well reproduced by the β-h model. In particular, the tendency of the β-h model to overestimate long-range spectral correlations in the XXZ spin chain is reversed in the case of the Bose-Hubbard model, indicating that this is a model-dependent feature.

V. RANDOM QUANTUM CIRCUIT

Consider a 1D chain of q-level systems of length L with the Floquet operator given by [77]

$$W_{a_1,\ldots,a_L;a_1',\ldots,a_L'} = U^{(1)}_{a_1,a_1'} \cdots U^{(L)}_{a_L,a_L'} e^{i\sum_n \varphi_{a_n',a_{n+1}'}}, \qquad (9)$$

where $U^{(j)}$ are unitary matrices that generate rotations at each site, chosen independently of the Haar distribution, and $\varphi_{a_n,a_{n+1}}$ are independent Gaussian random variables with zero mean and standard deviation ϵ that determine the coupling between neighboring sites. The SFF is related to the Floquet operator via $K(t) = \left\langle \mathrm{Tr}[W^t]\mathrm{Tr}[(W^\dagger)^t] \right\rangle$, where t is an integer and (5) is recovered with $g(\epsilon) = 1$ for $\tau \propto t$. The analytic calculation [77] in the limit $q \to \infty$ shows that the system is chaotic in the thermodynamic limit and SFF follows the prediction for GUE: $K(\tau) = 2\tau$. For $q = 3$, numerical calculations indicate that the system undergoes a transition between the ergodic phase at $\epsilon \gtrsim 0.25$, where the statistics of eigenphases θ_j are well described by GUE, and the MBL phase at $\epsilon \lesssim 0.25$, with PS statistics. We now turn to an analysis of level statistics of (9) at finite L and $q = 3$.

Distributions of higher-order spacing ratios (1) calculated for eigenphases θ_j are shown in Fig. 10. The β-h model with level repulsion exponent $\beta \in [0, 2]$ and an appropriately chosen range of interactions h reproduces the distributions of higher-order spacing ratios $P(r^{(n)})$, despite the broken time-reversal symmetry in the system. Average higher-order gap ratios for the random quantum circuit are shown in Fig. 11.

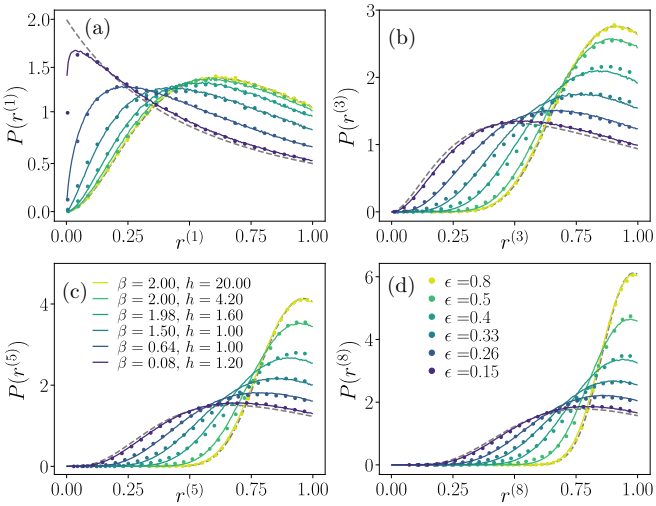

FIG. 10. Distributions of higher-order spacing ratios for model (9) with $L = 8$ and $q = 3$ for various ϵ are denoted by symbols. Lines correspond to the β-h model. Gray dashed lines correspond to $P(r^{(n)})$ distributions for GUE and PS.

The β-h model gives a good account of the spectral correlations reflected by $\Delta\bar{r}^{(n)}$. Notably, deviations at $n \gtrsim 20$ suggest also in this case that correlations between eigenphases of the Floquet operator W in the crossover regime are weaker than correlations predicted by the β-h model.

This suggests a similar behavior of level statistics at larger energy scales as in the case of the XXZ spin chain. Figure 12 shows the SFF of the considered Floquet operator (9) with predictions of the β-h model. The behavior of the SFF is qualitatively very similar to the case of the XXZ spin chain; $K(\tau)$ follows the prediction for GUE down to the Thouless time τ_{Th}, and for smaller τ, $K(\tau)$ flattens, matching SFF of the β-h model. On the ergodic side of the transition the SFF of the Floquet operator increases, indicating weaker correlations between eigenvalues than in the β-h model.

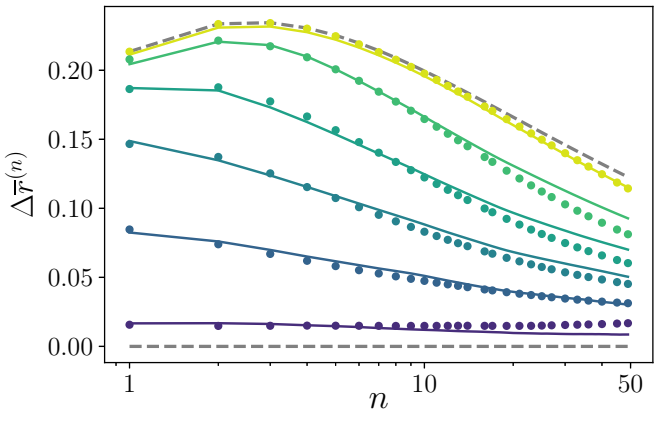

FIG. 11. The average higher-order spacing ratios $\Delta\bar{r}^{(n)}$ as a function of n for $\epsilon = 0.8, 0.5, 0.4, 0.33, 0.26, 0.15$ (from top to bottom) for the random quantum circuit are denoted by markers. Corresponding fits of the β-h model are denoted by solid lines; the β and h parameters are the same as in the text. Gray dashed lines correspond to $\Delta\bar{r}^{(n)}$ for GUE and PS.

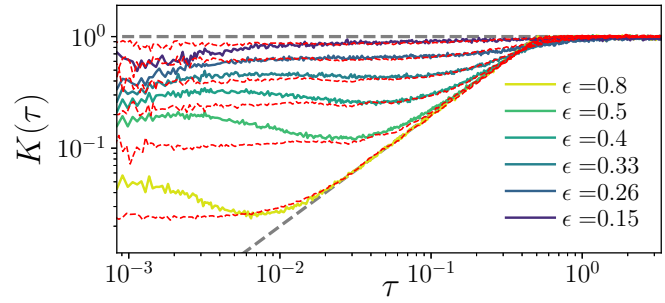

FIG. 12. SFF for the random circuit (9) of size $L = 8$ for various value of ϵ. Predictions of the β-h model with the same parameters as in Fig. 10 are denoted by red dashed lines. Gray dashed lines correspond to GUE and PS.

VI. DISCUSSION AND OUTLOOK

We have analyzed level statistics across the ergodic-MBL transition. The proposed β-h model provides a simple framework that allows one to reproduce universal features of level statistics of disordered interacting quantum many-body systems. The model captures the ergodic-MBL transition in the XXZ spin chain. Similarly, the β-h model is able to reproduce level statistics of disordered Bose-Hubbard models that undergo the ergodic-MBL transition [75,76]. The β-h model grasps also level statistics of the random quantum circuit across the transition between ergodic and MBL phases in spite of broken time-reversal symmetry. Notably, the only feature encoded in the Floquet operator (9) is the locality of gates in the circuit, and as such, the random circuit can be regarded as a toy model of a generic disorder interacting quantum system. All this taken together allows us to conjecture that the β-h model grasps universal, robust features of level statistics of interacting disordered quantum many-body systems, independent, for instance, of local conservation laws [77,78].

The transition between chaotic and integrable regimes in systems with chaotic classical counterparts [30,79] is system specific as it is determined by the structure of the underlying classical phase space [80]. Our analysis with the β-h model indicates that spectra of disordered interacting quantum many-body systems are effectively parametrized with good accuracy by only the level repulsion exponent β and the range of interactions between eigenvalues h, suggesting the existence of a robust mechanism of delocalization of LIOMs that ensure integrability and PS statistics in the MBL phase. A detailed understanding of such a mechanism remains an open problem. Spectral properties of disordered interacting many-body systems resemble level statistics at the single-particle Anderson localization transition [81,82] which could be expected as the MBL can be regarded as an Anderson localization in the Hilbert space [83–85].

The β-h model is capable of reproducing distributions of higher-order spacing ratios, level spacing distributions, and the number variance of systems across the ergodic-MBL transition. The range of interactions between eigenvalues h sets the Thouless time τ_{Th} at which the SFF deviates from the universal random matrix theory predictions. It would be interesting to compare this timescale to Thouless time extracted from matrix elements of local operators [86,87] or from the return probability [88]. The considered β-h model can also

be used to probe the entanglement spectrum in MBL systems [89] or random fractonic circuits [90], as it has been shown to host similar local correlations between energy levels. It would be interesting to relate it to the associated multifractality observed deep in the MBL phase [91] or to properties of level dynamics across the ergodic-MBL transition studied recently in [92].

ACKNOWLEDGMENTS

We are most grateful to F. Alet for kindly sharing with us the eigenvalues for the L=22,24 Heisenberg spin chain as well as discussions on subjects related to this work. We thank D. Delande for discussions and a careful reading of this paper. P.S. and J.Z. acknowledge support by PL-Grid Infrastructure. This research has been supported by the National Science Centre (Poland) under Projects No. 2015/19/B/ST2/01028 (P.S.), No. 2018/28/T/ST2/00401 (doctoral scholarship; P.S.), and No. 2016/21/B/ST2/01086 (J.Z.).

APPENDIX: REMARKS ON UNFOLDING

One of the advantages of the analysis of level statistics with higher-order spacing ratios $r^{(n)}$ is that they do not require spectral unfolding; that is, the level density $\rho(E)$ cancels out. This is, of course, valid only when n is such that $\rho(E_i)$ and $\rho(E_{i+2n})$ are not significantly different, which seems to be a plausible assumption when the dimension of the Hilbert space is larger than a few thousand.

The calculation of the SFF of the XXZ spin chain requires application of spectral unfolding. To this end we consider 40 000 eigenvalues from the center of the spectrum and fit the level staircase function [30] with a polynomial of degree 10. To calculate $K(\tau)$ we use $g(E) \propto \exp[-(E-\bar{E})^2/(0.18\Delta E^2)]$ (following [20]), where $\bar{E}$ is the average of the ground state and highest excited state energies and ΔE is the standard deviation of the energy in the given spectrum.

In order to obtain the level spacing distribution and the number variance of the XXZ spin chain we consider 500 eigenvalues from the middle of the spectrum, and we perform unfolding by fitting the level staircase function with a third-order polynomial.

Eigenphases θ_j of the random quantum Haar-measured circuit are distributed uniformly in the interval $[0, 2\pi]$; hence, no unfolding is required, and the SFF can be calculated directly from $K(t) = \langle \mathrm{Tr}[W^t]\mathrm{Tr}[(W^\dagger)^t] \rangle$.

[1] I. V. Gornyi, A. D. Mirlin, and D. G. Polyakov, Phys. Rev. Lett. **95**, 206603 (2005).
[2] D. Basko, I. Aleiner, and B. Altschuler, Ann. Phys. (NY) **321**, 1126 (2006).
[3] D. A. Huse, R. Nandkishore, and V. Oganesyan, Phys. Rev. B **90**, 174202 (2014).
[4] R. Nandkishore and D. A. Huse, Annu. Rev. Condens. Matter Phys. **6**, 15 (2015).
[5] F. Alet and N. Laflorencie, C. R. Phys. **19**, 498 (2018).
[6] D. A. Abanin, E. Altman, I. Bloch, and M. Serbyn, Rev. Mod. Phys. **91**, 021001 (2019).
[7] M. Serbyn, Z. Papić, and D. A. Abanin, Phys. Rev. Lett. **111**, 127201 (2013).
[8] V. Ros, M. Mueller, and A. Scardicchio, Nucl. Phys. B **891**, 420 (2015).
[9] J. Z. Imbrie, Phys. Rev. Lett. **117**, 027201 (2016).
[10] M. Mierzejewski, M. Kozarzewski, and P. Prelovšek, Phys. Rev. B **97**, 064204 (2018).
[11] M. Žnidarič, T. Prosen, and P. Prelovšek, Phys. Rev. B **77**, 064426 (2008).
[12] J. H. Bardarson, F. Pollmann, and J. E. Moore, Phys. Rev. Lett. **109**, 017202 (2012).
[13] Y. Bar Lev, G. Cohen, and D. R. Reichman, Phys. Rev. Lett. **114**, 100601 (2015).
[14] D. J. Luitz and Y. Bar Lev, Phys. Rev. Lett. **117**, 170404 (2016).
[15] M. Mierzejewski, J. Herbrych, and P. Prelovšek, Phys. Rev. B **94**, 224207 (2016).
[16] M. Schreiber, S. S. Hodgman, P. Bordia, H. P. Lüschen, M. H. Fischer, R. Vosk, E. Altman, U. Schneider, and I. Bloch, Science **349**, 842 (2015).
[17] J. Smith, A. Lee, P. Richerme, B. Neyenhuis, P. W. Hess, P. Hauke, M. Heyl, D. A. Huse, and C. Monroe, Nat. Phys. **12**, 907 (2016).
[18] J.-y. Choi, S. Hild, J. Zeiher, P. Schauß, A. Rubio-Abadal, T. Yefsah, V. Khemani, D. A. Huse, I. Bloch, and C. Gross, Science **352**, 1547 (2016).
[19] W. De Roeck and F. Huveneers, Phys. Rev. B **95**, 155129 (2017).
[20] J. Šuntajs, J. Bonča, T. Prosen, and L. Vidmar, arXiv:1905.06345.
[21] D. A. Abanin, J. H. Bardarson, G. D. Tomasi, S. Gopalakrishnan, V. Khemani, S. A. Parameswaran, F. Pollmann, A. C. Potter, M. Serbyn, and R. Vasseur, arXiv:1911.04501.
[22] P. Sierant, D. Delande, and J. Zakrzewski, arXiv:1911.06221.
[23] R. K. Panda, A. Scardicchio, M. Schulz, S. R. Taylor, and M. Žnidarič, Europhys. Lett. **128**, 67003 (2019).
[24] S. S. Kondov, W. R. McGehee, W. Xu, and B. DeMarco, Phys. Rev. Lett. **114**, 083002 (2015).
[25] H. P. Lüschen, P. Bordia, S. Scherg, F. Alet, E. Altman, U. Schneider, and I. Bloch, Phys. Rev. Lett. **119**, 260401 (2017).
[26] P. Roushan, C. Neill, J. Tangpanitanon, V. M. Bastidas, A. Megrant, R. Barends, Y. Chen, Z. Chen, B. Chiaro, A. Dunsworth, A. Fowler, B. Foxen, M. Giustina, E. Jeffrey, J. Kelly, E. Lucero, J. Mutus, M. Neeley, C. Quintana, D. Sank, A. Vainsencher, J. Wenner, T. White, H. Neven, D. G. Angelakis, and J. Martinis, Science **358**, 1175 (2017).
[27] A. Lukin, M. Rispoli, R. Schittko, M. E. Tai, A. M. Kaufman, S. Choi, V. Khemani, J. Léonard, and M. Greiner, Science **364**, 256 (2019).
[28] M. Rispoli, A. Lukin, R. Schittko, S. Kim, M. E. Tai, J. Léonard, and M. Greiner, Nature (London) **573**, 385 (2019).
[29] M. L. Mehta, *Random Matrices* (Elsevier, Amsterdam, 1990).
[30] F. Haake, *Quantum Signatures of Chaos* (Springer, Berlin, 2010).
[31] V. Oganesyan and D. A. Huse, Phys. Rev. B **75**, 155111 (2007).

[32] A. Pal and D. A. Huse, Phys. Rev. B **82**, 174411 (2010).
[33] L. F. Santos and M. Rigol, Phys. Rev. E **81**, 036206 (2010).
[34] R. Mondaini and M. Rigol, Phys. Rev. A **92**, 041601(R) (2015).
[35] D. J. Luitz, N. Laflorencie, and F. Alet, Phys. Rev. B **91**, 081103(R) (2015).
[36] D. J. Luitz, N. Laflorencie, and F. Alet, Phys. Rev. B **93**, 060201(R) (2016).
[37] J. Janarek, D. Delande, and J. Zakrzewski, Phys. Rev. B **97**, 155133 (2018).
[38] D. Wiater and J. Zakrzewski, Phys. Rev. B **98**, 094202 (2018).
[39] N. Macé, N. Laflorencie, and F. Alet, SciPost Phys. **6**, 050 (2019).
[40] P. Sierant, K. Biedroń, G. Morigi, and J. Zakrzewski, SciPost Phys. **7**, 008 (2019).
[41] N. Chavda, H. N. Deota, and V. K. B. Kota, Phys. Lett. A **378**, 3012 (2014).
[42] S. H. Tekur, U. T. Bhosale, and M. S. Santhanam, Phys. Rev. B **98**, 104305 (2018).
[43] V. K. B. Kota and N. D. Chavda, Int. J. Mod. Phys. E **27**, 1830001 (2018).
[44] U. T. Bhosale, arXiv:1905.02585.
[45] W. Buijsman, V. Cheianov, and V. Gritsev, Phys. Rev. Lett. **122**, 180601 (2019).
[46] J. M. G. Gómez, R. A. Molina, A. Relaño, and J. Retamosa, Phys. Rev. E **66**, 036209 (2002).
[47] P. Kos, M. Ljubotina, and T. Prosen, Phys. Rev. X **8**, 021062 (2018).
[48] B. Bertini, P. Kos, and T. Prosen, Phys. Rev. Lett. **121**, 264101 (2018).
[49] A. Chan, A. De Luca, and J. T. Chalker, Phys. Rev. X **8**, 041019 (2018).
[50] A. Chan, A. De Luca, and J. T. Chalker, Phys. Rev. Lett. **121**, 060601 (2018).
[51] P. Braun, D. Waltner, M. Akila, B. Gutkin, and T. Guhr, arXiv:1902.06265.
[52] E. Bogomolny, U. Gerland, and C. Schmit, Eur. Phys. J. B **19**, 121 (2001).
[53] A. Pandey, A. Kumar, and S. Puri, Phys. Rev. E **101**, 022217 (2020).
[54] A. Kumar, A. Pandey, and S. Puri, Phys. Rev. E **101**, 022218 (2020).
[55] W. K. Hastings, Biometrika **57**, 97 (1970).
[56] T. C. Berkelbach and D. R. Reichman, Phys. Rev. B **81**, 224429 (2010).
[57] K. Agarwal, S. Gopalakrishnan, M. Knap, M. Müller, and E. Demler, Phys. Rev. Lett. **114**, 160401 (2015).
[58] S. Bera, H. Schomerus, F. Heidrich-Meisner, and J. H. Bardarson, Phys. Rev. Lett. **115**, 046603 (2015).
[59] T. Enss, F. Andraschko, and J. Sirker, Phys. Rev. B **95**, 045121 (2017).
[60] S. Bera, G. De Tomasi, F. Weiner, and F. Evers, Phys. Rev. Lett. **118**, 196801 (2017).
[61] L. Herviou, S. Bera, and J. H. Bardarson, Phys. Rev. B **99**, 134205 (2019).
[62] L. Colmenarez, P. A. McClarty, M. Haque, and D. J. Luitz, SciPost Phys. **7**, 064 (2019).
[63] M. Serbyn and J. E. Moore, Phys. Rev. B **93**, 041424(R) (2016).
[64] C. L. Bertrand and A. M. García-García, Phys. Rev. B **94**, 144201 (2016).
[65] J. A. Kjäll, Phys. Rev. B **97**, 035163 (2018).
[66] P. Sierant and J. Zakrzewski, Phys. Rev. B **99**, 104205 (2019).
[67] F. Pietracaprina, N. Macé, D. J. Luitz, and F. Alet, SciPost Phys. **5**, 045 (2018).
[68] A. B. Harris, J. Phys. C **7**, 1671 (1974).
[69] J. T. Chayes, L. Chayes, D. S. Fisher, and T. Spencer, Phys. Rev. Lett. **57**, 2999 (1986).
[70] A. Chandran, C. R. Laumann, and V. Oganesyan, arXiv:1509.04285.
[71] T. Thiery, F. Huveneers, M. Müller, and W. De Roeck, Phys. Rev. Lett. **121**, 140601 (2018).
[72] A. Morningstar and D. A. Huse, Phys. Rev. B **99**, 224205 (2019).
[73] V. Khemani, S. P. Lim, D. N. Sheng, and D. A. Huse, Phys. Rev. X **7**, 021013 (2017).
[74] V. E. Kravtsov, I. V. Lerner, B. L. Altshuler, and A. G. Aronov, Phys. Rev. Lett. **72**, 888 (1994).
[75] P. Sierant, D. Delande, and J. Zakrzewski, Phys. Rev. A **95**, 021601(R) (2017).
[76] P. Sierant and J. Zakrzewski, New J. Phys. **20**, 043032 (2018).
[77] A. J. Friedman, A. Chan, A. De Luca, and J. T. Chalker, Phys. Rev. Lett. **123**, 210603 (2019).
[78] Y. Huang, arXiv:1902.00977.
[79] O. Bohigas, M. J. Giannoni, and C. Schmit, Phys. Rev. Lett. **52**, 1 (1984).
[80] O. Bohigas, S. Tomsovic, and D. Ullmo, Phys. Rep. **223**, 43 (1993).
[81] B. I. Shklovskii, B. Shapiro, B. R. Sears, P. Lambrianides, and H. B. Shore, Phys. Rev. B **47**, 11487 (1993).
[82] F. Evers and A. D. Mirlin, Rev. Mod. Phys. **80**, 1355 (2008).
[83] A. D. Luca and A. Scardicchio, Europhys. Lett. **101**, 37003 (2013).
[84] D. E. Logan and S. Welsh, Phys. Rev. B **99**, 045131 (2019).
[85] S. Ghosh, A. Acharya, S. Sahu, and S. Mukerjee, Phys. Rev. B **99**, 165131 (2019).
[86] D. J. Luitz and Y. B. Lev, Ann. Phys. (Berlin, Ger.) **529**, 1600350 (2017).
[87] M. Serbyn, Z. Papić, and D. A. Abanin, Phys. Rev. B **96**, 104201 (2017).
[88] M. Schiulaz, E. J. Torres-Herrera, and L. F. Santos, Phys. Rev. B **99**, 174313 (2019).
[89] S. D. Geraedts, R. Nandkishore, and N. Regnault, Phys. Rev. B **93**, 174202 (2016).
[90] S. Pai, M. Pretko, and R. M. Nandkishore, Phys. Rev. X **9**, 021003 (2019).
[91] N. Macé, F. Alet, and N. Laflorencie, Phys. Rev. Lett. **123**, 180601 (2019).
[92] A. Maksymov, P. Sierant, and J. Zakrzewski, Phys. Rev. B **99**, 224202 (2019).